Disease-toxicant screen reveals a nueroprotective interaction between Huntington's disease and manganese exposure

By: B. Blairanne Williams, Daphne Li, Michal Wegrzynowicz, Bhavin K. Vadodaria, Joel G. Anderson, Gunnar F. Kwakye, Michael Aschner, Keith M. Erikson, and Aaron B. Bowman

Williams, B.B., Vadodaria, B.K., Anderson, J.G., Kwakye, G.F., Li, D., Aschner, M., Erikson, K.M., Bowman, A.B. (2009) Disease-toxicant screen reveals a nueroprotective interaction between Huntington's disease and manganese exposure. Journal of Neurochemistry. ePub Oct 2009.

Made available courtesy of Wiley-Blackwell: http://www.wiley.com/

***** Note: Figures may be missing from this format of the document**
***** Note: The definitive version is available at http://www3.interscience.wiley.com**

Abstract:
Recognizing the similarities between Huntington's disease (HD) pathophysiology and the neurotoxicology of various metals, we hypothesized that they may exhibit disease-toxicant interactions revealing cellular pathways underlying neurodegeneration. Here, we utilize metals and the STHdh mouse striatal cell line model of HD to perform a gene–environment interaction screen. We report that striatal cells expressing mutant Huntingtin exhibit elevated sensitivity to cadmium toxicity and resistance to manganese toxicity. This neuroprotective gene–environment interaction with manganese is highly specific, as it does not occur with iron, copper, zinc, cobalt, cadmium, lead, or nickel ions. Analysis of the Akt cell stress signaling pathway showed diminished activation with manganese exposure and elevated activation after cadmium exposure in the mutant cells. Direct examination of intracellular manganese levels found that mutant cells have a significant impairment in manganese accumulation. Furthermore, YAC128Q mice, a HD model, showed decreased total striatal manganese levels following manganese exposure relative to wild-type mice. Thus, this disease-toxicant interaction screen has revealed that expression of mutant Huntingtin results in heightened sensitivity to cadmium neurotoxicity and a selective impairment of manganese accumulation.
Keywords: gene–environment Interactions,Huntington's disease, manganese, neurodegeneration, neuroprotection, neurotoxicity.

Article:
In Huntington's disease (HD), degeneration of the medium spiny neurons within the corpus striatum occurs well prior to other affected brain regions such as the cortex (Imarisio et al. 2008). This selective degeneration occurs despite widespread expression of the disease-causing, polyglutamine-expanded protein, huntingtin (HTT). Thus, other factors within the striatum may uniquely increase the vulnerability of this area to the pathophysiological mechanisms of HD. Interestingly, the toxicant 3-nitroproprionic acid (3NPA), a mitochondrial complex II inhibitor, exhibits an HD-like striatal specific neurodegeneration (Beal et al. 1993). One explanation of this common pathology is that both mutant HTT and 3NPA might impinge upon a shared pathophysiological vulnerability inherent to the striatum. Indeed, both HD and 3NPA toxicity cause mitochondrial dysfunction, oxidative stress, excitotoxicity, and altered iron and copper homeostasis (Dexter et al. 1991; Fox et al. 2007; Simmons et al. 2007).

We postulate that toxicants acting upon pathophysiological targets modulated in HD will exhibit disease-toxicant interactions, even if patients are not normally exposed to these toxicants. Furthermore, the identification of these interactions may uncover mechanisms of selective neurodegeneration because of environmental or genetic factors. Therefore, a disease-toxicant interaction screen may facilitate the identification of toxicants with common pathophysiological targets or mechanisms. The toxicological properties of metals are diverse, and include oxidative stress, deranged calcium signaling, activation of cell stress pathways, protein aggregation, and altered energy metabolism (Bush 2000; Zecca et al. 2004). Here, we exploit this broad toxicology to screen for gene–environment interactions between neurotoxic metals and the

glutamine-expanded disease-causing HTT protein. We report the surprising discovery that expression of mutant HTT protects against manganese toxicity in part by substantially decreasing manganese accumulation during exposure.

Materials and methods

Chemicals, reagents, and cell culture supplies

Cell culture media and supplements were obtained from Mediatech (Manassas, VA, USA) unless indicated. Cell lines were grown in Dulbecco's modified Eagle's medium with 10% fetal bovine serum (Atlanta Biologicals, Lawrenceville, GA, USA), L-glutamine, 400 µg/mL G418, and penicillin–streptomycin. Metals and toxicants used in survival assays were from Alfa Aesar (Ward Hill, MA, USA) unless indicated: 3NPA (Sigma, St Louis, MO, USA), Fe(III) chloride (VWR, West Chester, PA, USA), Mn(II) chloride, Cd(II) chloride, Co(II) chloride, Cu(II) chloride, Pb(II) chloride, Ni(II) sulfate, and Zn(II) chloride. Buffers and solutions for assays: 3-(4,5-dimethylthiazol-2-yl)-2,5-diphenyltetrazolium bromide (MTT) salt (VWR), Sorenson's buffer (0.1 M glycine and 0.1 M $NaCl_2$, pH 10.5), dimethyl sulfoxide (DMSO; Sigma). Phosphate-buffered saline (PBS) with 0.1% Triton X-100 (Sigma); 4% p-formaldehyde in PBS (diluted from 16% solution; Electron Microscopy Sciences, Hatfield, PA, USA) were used for cell imaging studies.

Antibodies

Antisera for western blotting include HTT (2166) 1 : 20 000 (Millipore, Billerica, MA, USA), Pan Akt 1 : 1000 (Cell Signaling, Beverly, MA, USA), phospho-Akt 1 : 1000 (Cell Signaling), and actin 1 : 2000 (Developmental Studies Hybridoma Bank, Iowa City, IA, USA). Appropriate secondary antibodies from Jackson Immunoresearch Laboratories (West Grove, PA, USA) were used at 1 : 15 000 accordingly.

Cell survival assays

The clonal striatal cell lines – both mutant $STHdh^{Q111/Q111}$ and wild-type $STHdh^{Q7/Q7}$ – were a generous gift from Marcy Macdonald, PhD (Massachusetts General Hospital, Boston, MA, USA), and grown at 33°C (Cattaneo and Conti 1998; Trettel et al. 2000). $STHdh^{Q111/Q111}$ and wild-type $STHdh^{Q7/Q7}$ cells were plated at equal density the evening before treatment. Toxins or metals were added to the culture media the next morning and cells were exposed for 26–30 h. Cell viability was assessed by either trypan blue exclusion or MTT assay. Briefly, trypan blue exclusion – cells were harvested after exposure to various metals by trypsinization and exposed to trypan blue following published protocol (Ying et al. 2000). MTT assays were performed according to established protocols (Ehrich and Sharova 2000). Briefly, culture media was removed, and 500 µL of 0.5% MTT salt in minimal essential medium (Invitrogen, Carlsbad, CA, USA) containing fetal bovine serum and penicillin–streptomycin was added to each well for 4 h. Next, the minimal essential medium was removed and Sorenson's buffer was diluted 2.5 mL into 20 mL of DMSO; 200 µL of Sorenson's buffer in DMSO was added to the empty wells to dissolve the precipitate. The plates were returned to the incubator until all the MTT salt precipitate could no longer be visualized under a microscope; 60 µL from each well was removed and placed in a 96-well plate and absorbance was read at 570–590 nm. Cell survival data were normalized by genotype to the vehicle-only exposed control included in each independent sample set.

Mutant HTT expression construct

The polyglutamine expansion of 128 repeats was created by PCR of the CAG repeat from the YAC128Q mouse model and subcloned into a full-length HTT cDNA construct (gift from Juan Botas, Baylor College of Medicine, Houston, TX, USA). The new full-length mutant HTT cDNA was then subcloned into pCDNA3.1 (Invitrogen), a mammalian expression vector to make full-length HTT with 128 glutamines in the polyglutamine domain (HTT[128Q]), mammalian expression construct (pHTT[128Q]). A control construct containing the full-length HTT cDNA in the reverse orientation, was used as a control vector in transfection experiments to control for the large size of pHTT[128Q] vector. The inverted control does not express the HTT protein, confirmed by western blot analysis (data not shown).

Cell viability analysis in transfected cells

Equal numbers of wild-type STHdh$^{Q7/Q7}$ cells were plated onto glass coverslips ~10 h prior to transfection using lipofectAMINETM 2000 (Invitrogen). The pEGFP-N1 expression vector (Invitrogen) was co-transfected with pHTT[128Q] or the control vector at a 1 : 3 ratio to allow estimates of transfection efficiencies. Approximately 70% of cells were green fluorescent protein (GFP) positive. Cells were treated with $MnCl_2$ 24 h post-transfection and analyzed 30 h after exposure. Coverslips were harvested, washed in PBS with 0.1% Triton X-100, fixed with 4% p-formaldehyde, washed again, and mounted onto slides with ProLong Gold antifade reagent with 4',6-diamidino-2-phenylindole (DAPI) nuclear stain (Invitrogen). 4',6-diamidino-2-phenylindole (DAPI)-positive cells were imaged by fluorescence microscopy using a Zeiss Axioplan microscope (Thornwood, NY, USA) with a 10x objective by systematic unbiased sampling of non-overlapping fields. Number of surviving cells per field was quantified using NIH ImageJ (Bethesda, MD, USA) by the threshold and analyze particles commands as previously described (Bowman et al. 2007).

Westerns blot

Equal numbers of wild-type and mutant STHdh cells were plated and treated with Mn(II) or Cd(II) for 3 or 30 h. The cell pellets were lysed in lysis buffer [50 mM Tris, 150 mM $NaCl_2$, 0.1% sodium dodecyl sulfate (SDS), 1.0% Nonidet 40, 12 mM deoxycholic acid, 1x protease inhibitor cocktail (Sigma), and 1x phosphatase inhibitor cocktails I and II (Sigma)], and loaded by equal cell number or protein for sodium dodecyl sulfate–polyacrylamide gel electrophoresis. Western blots were visualized with Thermo Scientific Pierce Supersignal West Dura Extended Duration Chemiluminescent Substrate (Waltham, MA, USA) on an Ultralum Omega 12iC (Claremont, CA, USA). Measurements of integrated density of protein bands was performed using ImageJ (NIH), with background correction calculated using a signal ratio error model, as described (Kreutz et al. 2007). Calculations of relative signal were normalized to untreated wild-type or mutant sample for each set, as indicated.

Animal manganese exposure

All animal studies strictly followed protocols approved by the Vanderbilt University Institutional Animal Care and Use Committee and were adopted to minimize pain and distress of the animals. The FVB-Tg(YAC128)53Hay/J mouse line (YAC128Q) was obtained from JAX (#004938, Bar Harbor, ME, USA) (Slow et al. 2003). The manganese-exposure protocol followed a previously published paradigm (Dodd et al. 2005). In brief, 3-month-old YAC128Q HD mutant mice and their wild-type littermates were injected subcutaneously with 50 mg/kg manganese chloride tetrahydrate. All injections were carried out blind to genotype. Injections were carried out on Days 0, 3, and 7. On Day 8, the animals were killed by cervical dislocation, the brain regions were dissected, tails clipped for genotyping, and trunk blood collected into heparin coated tubes. Tissue collection and graphite furnace atomic absorption spectroscopy (GFAAS) were performed blind to both genotype and exposure. The tissues were then flash-frozen for analysis of manganese content. Analysis of manganese content by GFAAS was performed blind to genotype and exposure. Genotyping was carried out according to a previously published method (#004938; from JAX) (Slow et al. 2003).

Graphite furnace atomic absorption spectroscopy

Manganese and iron concentrations were measured with GFAAS (AA240; Varian Inc., Palo Alto, CA, USA). STHdh cells were cultured and treated as described above for cell viability assays, harvested by trypsinization, washed multiple times in PBS and then flash-frozen until analysis. For analysis, cell pellets were thawed and digested in 200 µL ultrapure nitric acid for 24 h in a sandbath (60°C). Brain tissue samples were diluted 1 : 5 (weight to volume) in 1x PBS and sonicated for 30 s. For protein analysis of the tissue samples, a 10 µL aliquot of the tissue homogenate was combined with 10 µL of lysis buffer. Homogenates were incubated on ice for 20 min before being centrifuged at 10 000 g for 20 min at 4°C. The supernatant was then transferred to new tubes, and the total protein concentration was determined by bicinchoninic acid assay (Pierce, Rockford, IL, USA). An equal volume of ultrapure nitric acid was then added to the remaining homogenate and the sample was digested for 48 h in a sandbath (60^0C). Manganese content was determined by the following protocol: A 20 µL aliquot of the digested sample was brought to 1 mL total volume with 2% nitric acid for analysis. Bovine liver (NBS Standard Reference Material; USDC, Washington, DC, USA) (10 µg Mn/g) was digested in ultrapure

nitric acid and used as an internal standard for analysis (final concentration 10 µg Mn/L) as published previously (Anderson et al. 2009).

Statistical analysis

Univariate, multivariate, and repeated measures ANOVA were performed using SPSS software (SPSS, Inc., Chicago, IL, USA). Post hoc analysis and pair-wise comparisons were performed using Microsoft Excel (Redmond, WA, USA) by Student's t-tests (two-tailed), except for comparison of normalized data versus control which were performed by testing for non-overlap of the 95% confidence interval, error bars are expressed as SEM. Animal manganese-exposure data were analyzed by multivariate ANOVA using blood manganese levels as a covariate. The alpha level for all of the analyses was set at $p \leq 0.05$.

Results

Huntington's disease-toxicant interaction screen

To establish a gene–environment interaction model between metals and mutant htt, we utilized the HD mouse striatal cell line model developed by Marcy Macdonald. The model shares many phenotypic similarities with HD mouse models and human patients (Trettel et al. 2000; Imarisio et al. 2008). The striatal cell lines express full-length (wild-type or glutamine expanded) htt from the endogenous locus allowing comparisons of phenotypes between wild-type ($STHdh^{Q7/Q7}$) and mutant ($STHdh^{Q111/Q111}$) cells. The initial screen focused on cell survival as a basic toxicological phenotype. Previous research by Macdonald and colleagues has shown that the mutant cell line ($STHdh^{Q111/Q111}$) line has increased sensitivity to the toxicant 3NPA (Ruan et al. 2004). Therefore, as a positive control, we examined cell survival in the striatal cell model following 30 h exposure to 3NPA. We confirmed that the mutant $STHdh^{Q111/Q111}$ line has a significant ($p < 0.05$) decrease in cell survival relative to wild-type cells after 3NPA exposure (Fig. S1).

After validating the HD striatal model for detection of gene–environment interactions relevant to HD, we initiated a cell survival screen to determine whether expression of mutant htt modulates sensitivity to a diverse set of metal toxicants. We screened eight neurotoxic metal ions, Fe(III), Cu(II), Pb(II), Co(II), Zn(II), Ni(II), Cd(II), and Mn(II), by generating concentration–response curves (Fig. 1). Metal concentrations were chosen to generate a survival curve spanning non-toxic to highly toxic exposures. We were unable to induce a high degree of cell death (> 40%) for Fe(III) and Pb(II) because of the insufficient solubility of these metals at higher concentrations. Nevertheless, statistical analysis of cell survival by two-way ANOVA revealed a significant effect of exposure on cell survival for each of the eight metals ($p < 0.001$). Wild-type and mutant STHdh cell line survival curves were indistinguishable for Fe(III), Cu(II), Pb(II), Co(II), Zn(II), and Ni(II) (Fig. 1). In contrast, Cd(II) and Mn(II) both showed differential effects on wild-type and mutant cell survival (Fig. 1). The mutant $STHdh^{Q111/Q111}$ cells displayed an increased sensitivity to Cd cytotoxicity. Statistical analysis by two-way univariate ANOVA found a significant effect of genotype [$F_{(1,29)} = 5.3\ 1$, $p = 0.029$] on cell survival. Post hoc analysis indicated that the wild-type line had significantly ($p < 0.05$) higher survival at 50 µM Cd(II) relative to mutant cells (Fig. 1). Analyses of Mn(II) toxicity in the STHdh cells revealed an unexpected gene–environment interaction, in which cells expressing mutant htt were resistant to Mn(II) toxicity. Statistical analysis by two-way repeated measures ANOVA found a significant effect of genotype [$F_{(1,8)} = 323.2$, $p < 0.001$] on cell survival.

Post hoc analysis indicated that the mutant line had significantly ($p < 0.01$) higher survival at 50, 100, and 300 µM Mn(II) relative to wild-type cells (Fig. 1).

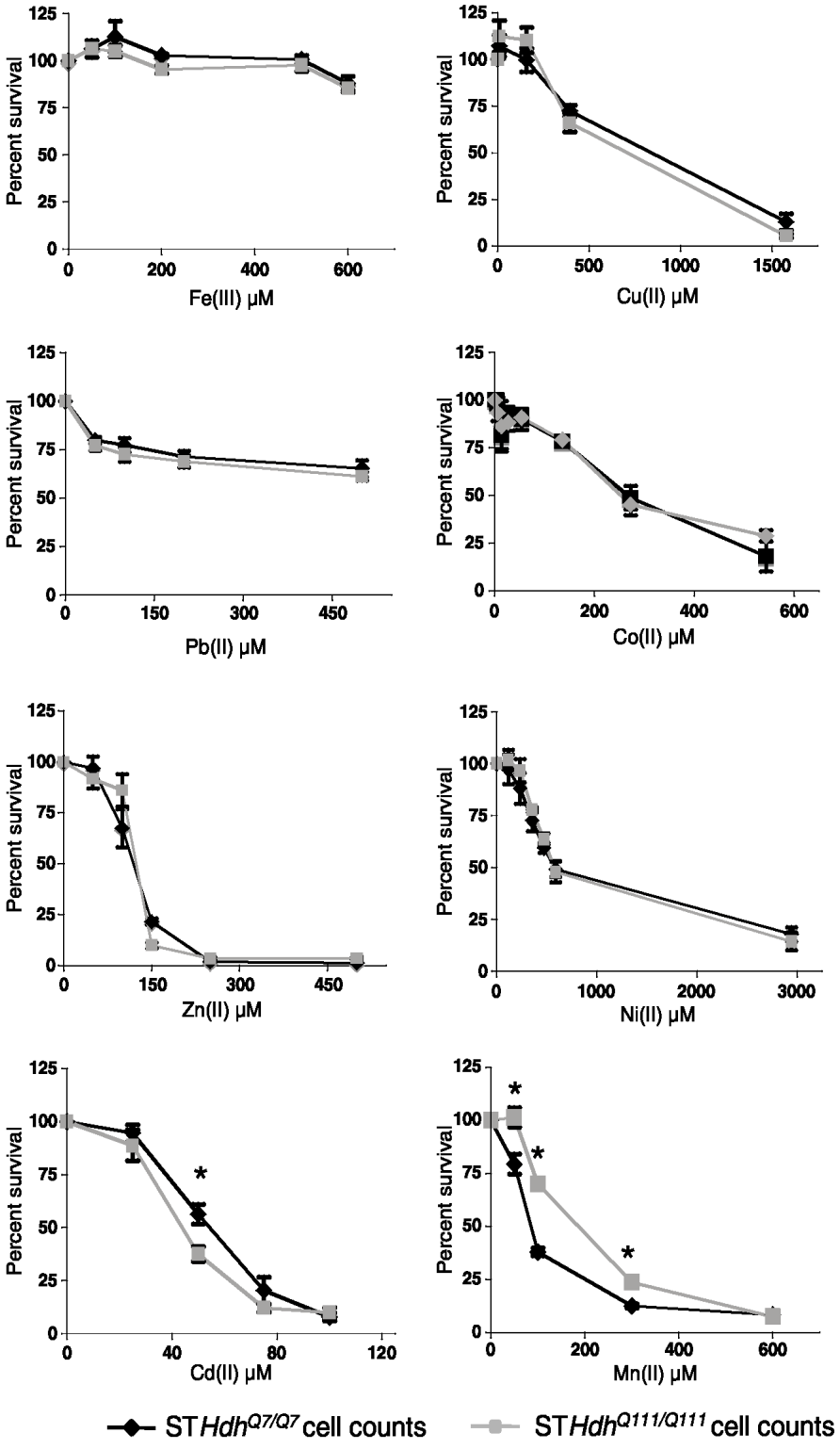

Fig. 1 Huntington's disease – metal toxicity cell survival screen. Equal numbers of wild-type ST*Hdh*$^{Q7/Q7}$ (black) or mutant ST*Hdh*$^{Q111/Q111}$ (gray) cells were exposed to the indicated metal ions. Cell survival was assessed 26–30 h after exposure by MTT assay for all metals except Cu, which was assessed by trypan blue exclusion. The average absorbance (or mean cell counts for Cu) relative to the untreated control for each genotype is plotted as percent cell survival (± SEM), with Cu(II) chloride (four experiments), Fe(III) chloride (three experiments), Cd(II) chloride (four experiments), Zn(II) chloride (three experiments), Pb(II) chloride (three experiments), Co(II) chloride (four experiments), Ni(II) chloride (three experiments), and Mn(II) chloride (two experiments). Each experiment had between three and six independent samples at each genotype/metal concentration point; ANOVA showed a significant effect of exposure on cell survival for all metals ($p < 0.001$), and finds a significant difference in cell survival between genotypes only for Cd(II) ($p = 0.029$) and Mn(II) ($p = 0.001$). Significant differences in survival (*$p < 0.05$ *post hoc t*-test) between wild-type and mutant cells at specific exposure levels are shown.

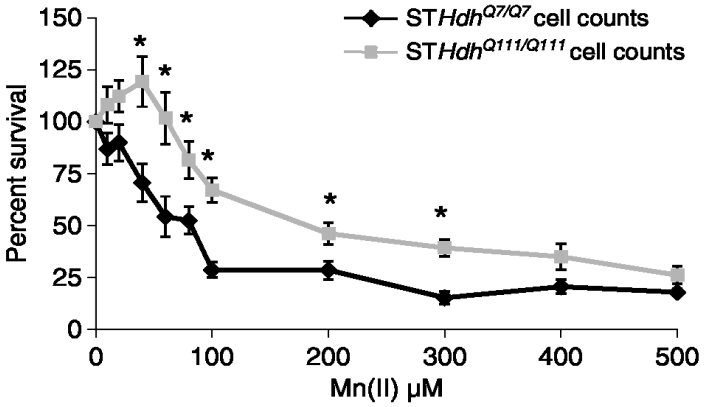

Fig. 2 Mutant HD striatal cells are resistant to Mn(II) cytotoxicity. Equal numbers of wild-type ST*Hdh*$^{Q7/Q7}$ (black) or mutant ST*Hdh*$^{Q111/Q111}$ (gray) cells were exposed to increasing concentrations of manganese chloride. Cell survival was assessed 30 h after exposure by trypan blue exclusion assay. The percent of viable cells relative to the untreated control is shown (± SEM, $n = 3$ independent experiments). Significant differences in survival (*$p < 0.05$ *post hoc t*-test) between wild-type and mutant cells are shown.

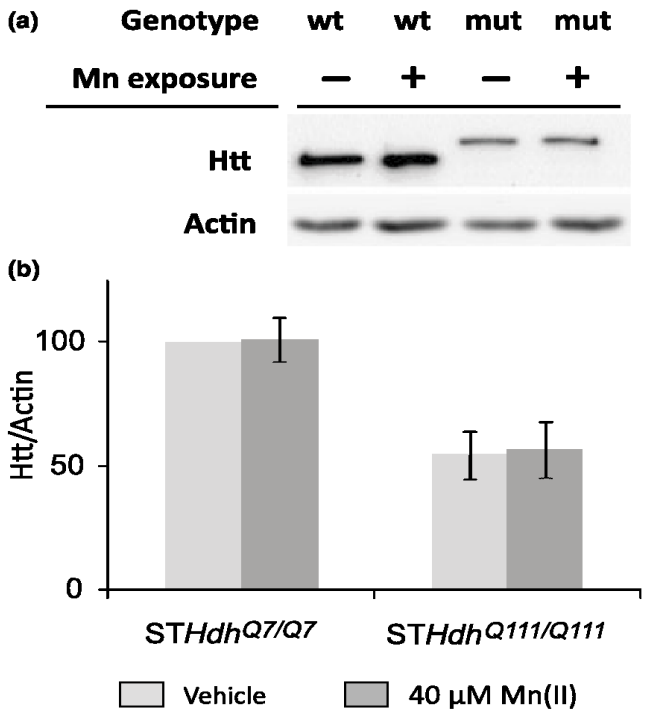

Fig. 3 Mn(II) exposure does not alter htt protein levels in striatal cells. (a) representative blot showing lysates from ST*Hdh*$^{Q7/Q7}$ (wt) or ST*Hdh*$^{Q111/Q111}$ (mut) cells after 30 h of 40 µM Mn(II) chloride exposure (+) were analyzed by western blot. The htt protein from mutant animals runs at a higher molecular weight because of the glutamine-tract expansion. (b) Quantification of htt protein expression in striatal cell lines relative to actin. Mean values are plotted as a percentage of the vehicle exposed wild-type cells (± SEM, $n = 7$ independent samples). Statistical analysis of htt protein levels by two-way univariate ANOVA found a significant effect of genotype [$F_{(1,28)} = 28.1$, $p < 0.001$], but indicated no significant effect of Mn(II) exposure [$F_{(1,28)} = 1.13$, $p = 0.298$] or a genotype by exposure interaction [$F_{(1,28)} = 1.16$, $p = 0.292$]. Significant differences in htt protein levels between genotypes were detected for both vehicle and Mn(II) exposed cells ($p < 0.05$ *post hoc t*-test).

Mn(II) survival curve

The MTT assay used in the initial screen is an indirect measure of cell survival. To determine if the HD-manganese interaction observed by MTT assay was directly because of changes in cell survival we used the trypan blue exclusion assay (Fig. 2). This independent and expanded survival curve for Mn(II) confirmed that the gene–environment interaction seen by MTT assay was due to changes in cell survival rather than just differences in mitochondrial reductase activity (Figs 1 and 2). Statistical analysis by two-way univariate ANOVA found a significant effect of genotype [$F_{(1,88)} = 59.3$, $p < 0.00\ 1$] on cell survival with Mn(II) exposure, in addition a two-way interaction between genotype and Mn(II) exposure was detected [$F_{(10,88)} = 2.1$, $p = 0.039$] indicating that each genotype had a unique Mn-response curve. Over a broad range of Mn(II) exposures (40–300 µM) the HD mutation limited Mn(II) cytotoxicity of the metal when compared with the wild-type cell line ($p < 0.05$). At the highest concentrations of Mn(II) tested (400–500 µM), the toxicity is not significantly different between wild-type and mutant cell lines. Therefore, the survival curve for Mn(II) shows a gene– environment interaction wherein mutant htt counters the toxic effects of Mn(II) exposure.

40 µM Mn(II) exposure does not significantly alter htt protein levels

The htt gene has been shown to be Fe-responsive (Hilditch-Maguire et al. 2000) and Mn(II) exposure is known to alter cellular Fe levels (Zheng et al. 1999). To test the hypothesis that manganese exposure might influence cell viability by altering htt protein levels, we used western blot analysis to measure mutant and wild-type htt levels in the HD cell model (Fig. 3a). Quantitative analysis demonstrated that htt levels were not significantly altered in wild-type or mutant striatal cells after exposure to 40 µM Mn(II) for 30 h (Fig 3b). As previously reported, mutant htt levels are decreased in the STHdh$^{Q111/Q111}$ cells relative to wild-type protein levels in the wild-type cell line (Fig. 3) (Trettel et al. 2000).

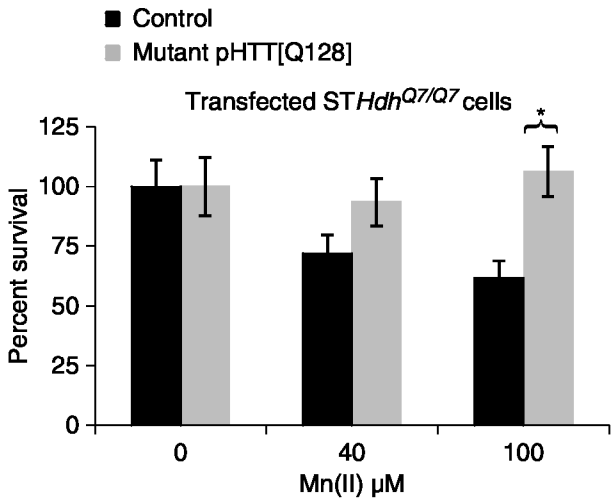

Fig. 4 Expression of mutant *HTT* confers Mn-resistance phenotype. The vectors pHTT[128Q] and pEGFP-N1 were transiently expressed in the ST*Hdh*$^{Q7/Q7}$ cell line and compared with a control vector plus pEGFP-N1 transfection. Following exposure to Mn(II) chloride for 30 h, cells were stained with DAPI then analyzed by fluorescence microscopy. The number of surviving cells per visual field (18 images per transfection/exposure group, nine images from two independent coverslips) was counted by automated image analysis using NIH ImageJ software. Mean values are plotted as the percentage of cells relative to the average number of cells (± SEM) in vehicle exposed controls for each transfection condition, $n = 18$ images. Significant differences in survival (*$p < 0.05$ *post hoc t*-test) between *HTT[128Q]* expressing and control cells are indicated.

Expression of mutant HTT is sufficient for the manganese-resistance phenotype

The wild-type and mutant striatal cell lines are independent lines. Thus, differences in their response to Mn(II) exposure might be because of expression of mutant htt or other inherent differences between the two lines. To determine if the Mn(II) resistance phenotype is due to expression of mutant htt we transiently transfected full-

length human mutant HTT with 128 repeats (HTT[128Q]) or a control vector into the wild-type STHdh$^{Q7/Q7}$ cells. Transfected cells were exposed to vehicle, 40 μM Mn(II), or 100 μM Mn(II) and cell survival assessed by microscopy (Fig. 4). Statistical analysis by two-way univariate ANOVA revealed a significant difference between HTT[128Q] and control transfected cells [$F_{(1,108)} = 7.33$, $p = 0.008$] and a significant two-way interaction between Mn(II) exposure and transfection [$F_{(2,108)} = 3.92$, $p = 0.023$]. Post hoc analysis indicated significantly higher cell survival following Mn(II) exposure in the HTT[128Q] transfected cells relative to control cells (Fig. 4). Therefore, expression of mutant HTT is sufficient to confer resistance to manganese toxicity.

Diminished Mn(II)-dependent Akt activation in HD striatal cells

As changes in S473-phosphorylated Akt (S473-P-Akt) levels are associated with both Mn(II) toxicity and HD, we hypothesized that this signaling pathway would show disease-toxicant interactions (Humbert et al. 2002; Gines et al. 2003a; Colin et al. 2005; Warby et al. 2005; Bae et al. 2006; Liao et al. 2007; Lee et al. 2009). To begin we quantified S473-P-Akt levels following a 30-h exposure to 40 μM Mn(II). This exposure led to a manganese-dependent increase in S473-P-Akt levels ($p < 0.05$) in wild-type cells, yet mutant cells showed no detectable change in S473-PAkt levels relative to untreated mutant cells (data not shown). As expected from previous work, S473-P-Akt levels were elevated in the mutant line versus wild-type (Gines et al. 2003a). Thus, the lack of a manganese-dependent increase in S473-P-Akt in the mutant cells might be because of a general inability of these cells to increase S473-P-Akt levels beyond their already higher basal levels. To determine if higher levels of Mn(II) are capable of increasing S473-P-Akt levels, we exposed cells for a shorter time point (3 h) to allow us to collect protein before significant cell death. At this time point, other studies reported strong manganese-dependent increases in S473-PAkt levels (Bae et al. 2006; Lee et al. 2009). We found that mutant STHdh$^{Q111/Q111}$ cells were capable of increasing S473-P-Akt levels in response to high concentrations of Mn(II). However, while 40 μM Mn(II) was sufficient to significantly raise S473-P-Akt above basal levels in wild-type cells ($p < 0.05$), we did not detect a significant increase in S473-P-Akt above its higher basal levels in mutant cells until 200 μM Mn(II) or higher ($p < 0.05$) (Figs 5 and S2). Interestingly, at exposures of 100 μM and above, the levels of S473-P-Akt in the wild-type cells increased sufficiently to equal the levels seen in mutant cells exposed at the same Mn(II) concentration (Fig. S2). Controlling for the elevated S473-P-Akt levels in the mutant cells by normalizing the basal levels of each genotype to 100%, mutant cells exhibited a significant decrease in S473-P-Akt activation relative to wild-type cells across all tested Mn(II) concentrations ($p < 0.05$) (Fig. 5).

Enhanced Cd(II)-dependent Akt activation in HD striatal cells

To evaluate whether the differential phosphorylation of Akt following Mn(II) exposure in mutant cells is a specific marker of the manganese-HD interaction, we tested the effect of Cd(II) exposure on S473-P-Akt levels in the STHdh cell lines. We chose to test cadmium given its opposite effect from manganese on cell survival (Fig 1). Published evidence has demonstrated that Cd(II) exposure leads to phosphorylation of Akt at S473 in a variety of cell types (Thevenod 2009). A 3-h exposure of STHdh cells to 50 μM Cd(II) increased S473-P-Akt levels in both wild-type and mutant lines (Figs 5 and S2). Indeed, despite the elevated basal levels of S473-P-Akt, Cd(II) exposed mutant STHdh$^{Q111/Q111}$ cells had significantly higher levels of S473- P-Akt than wild-type cells ($p < 0.05$) (Fig. S2). Controlling for the difference in basal S473-P-Akt levels, mutant and wild-type cells both had a similar approximately twofold increase in S473-P-Akt levels (Fig. 5). Thus, the elevated basal S473-P-Akt levels in the mutant cells do not limit per se the capacity of mutant cells to increase the S473-P-Akt to total Akt ratio.

Cellular manganese accumulation is substantially impaired by mutant htt

Given the severely blunted S473-P-Akt response of the mutant cells to Mn(II) exposure, we tested the hypothesis that the expression of mutant htt impedes the cellular stress response to Mn(II) by decreasing accumulation of manganese during exposure. We measured total intracellular manganese and iron levels following Mn(II) exposure in the STHdh$^{Q7/Q7}$ and STHdh$^{Q111/Q111}$ cell lines by GFAAS (Garcia et al. 2007). We observed that the STHdh$^{Q111/Q111}$ cells accumulated fourfold ($p < 0.005$) and 10-fold ($p < 0.001$) less manganese after a 30-h exposure to 40 μM Mn(II) and 100 μM Mn(II), respectively (Fig. 6a).

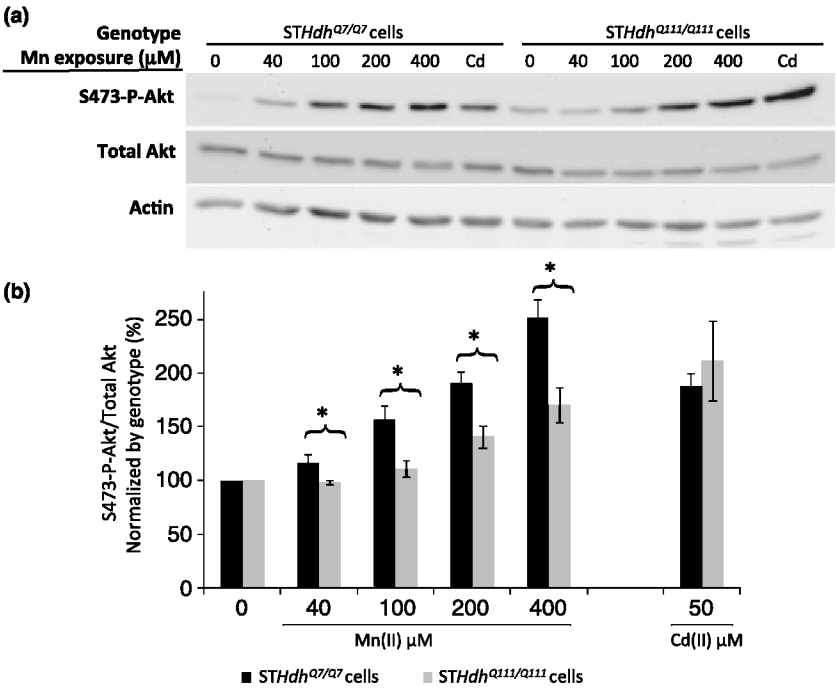

Fig. 5 Diminished manganese-dependent Akt phosphorylation in HD striatal cells. (a) Lysates harvested from ST*Hdh*$^{Q7/Q7}$ (wild-type) or ST*Hdh*$^{Q111/Q111}$ (mutant) cells after 3 h of manganese chloride exposure were analyzed by western blot for phosphorylated Akt (S473-P-Akt), total Akt, and actin. Representative blots are shown. (b) Quantification of S473-P-Akt/total Akt expression in striatal cell lines. Mean values were normalized by genotype to the vehicle-only control (± SEM, $n = 4$ independent samples). Significant differences in protein levels (*$p < 0.05$ *post hoc* *t*-test) between genotypes are indicated for each exposure.

No difference in basal manganese levels was seen, however, the manganese levels in the vehicle-only samples were near the lower detection limit of the GFAAS. Examination of total iron levels in these cells revealed no differences between wild-type and mutant cells at basal state or 40 μM Mn(II) exposure, though wild-type cells showed a trend toward elevated total iron at the 100 μM Mn(II) exposures ($p = 0.13$) not seen in the mutant cells (Fig. 6b). Thus, differences in manganese accumulation between wild-type and mutant cells did not correlate with significant changes in iron accumulation.

Striatal specific deficit in total manganese accumulation in YAC128Q HD mouse model

To determine if expression of mutant HTT influences manganese accumulation in vivo, we exposed 3-month (presymptomatic) YAC128Q HD mice and wild-type litter-mates to Mn(II) using a subcutaneous manganese-exposure paradigm (Slow et al. 2003; Dodd et al. 2005). Loss of striatal volume in the YAC128Q HD mouse model is absent as late as 6 months of age, and is first detected at 9 months of age (Slow et al. 2003). Analyses of cerebellar, cortical, hippocampal, and striatal manganese levels by GFAAS indicated that Mn(II) exposed wild-type animals had increased total manganese levels in all four brain regions with the striatum having the greatest accumulation (Fig. 7). Cerebellum, cortex and hippocampus showed similar increases in manganese levels between wild-type and mutant animals, while striatum from wild-type Mn(II) exposed animals showed higher levels than mutant (1.51 vs. 0.92 nmol Mn/mg protein). A multivariate two-way ANOVA was used to analyze regional manganese levels (Table S1). ANOVA found a significant effect of Mn(II) exposure for each of the four brain regions ($p < 0.05$). A significant effect of genotype and a genotype by exposure two-way interaction was found for striatum only ($p < 0.05$). Post hoc analysis of striatal manganese levels showed significantly less ($p < 0.05$) manganese accumulation in mutant versus wild-type Mn(II) exposed animals (Fig. 7). We also examined iron levels in the same brain tissues. Data were analyzed by multivariate two-way ANOVA model (Fig. S3 and Table S2). This analysis failed to find a significant effect of Mn(II) exposure or a two-way genotype by Mn(II) exposure interaction for iron levels in any brain region, though a significant genotype difference in cerebellar iron levels was seen ($p = 0.024$). Finally, we have confirmed the impaired striatal manganese accumulation in the YAC128Q HD animals in an independent set of animals by inductively coupled plasma mass spectrometry (data not shown). Therefore, a mouse model of HD that recapitulates the selective degeneration of the corpus striatum observed in patients, also exhibited an early and selective deficit in striatal manganese accumulation after Mn(II) exposure.

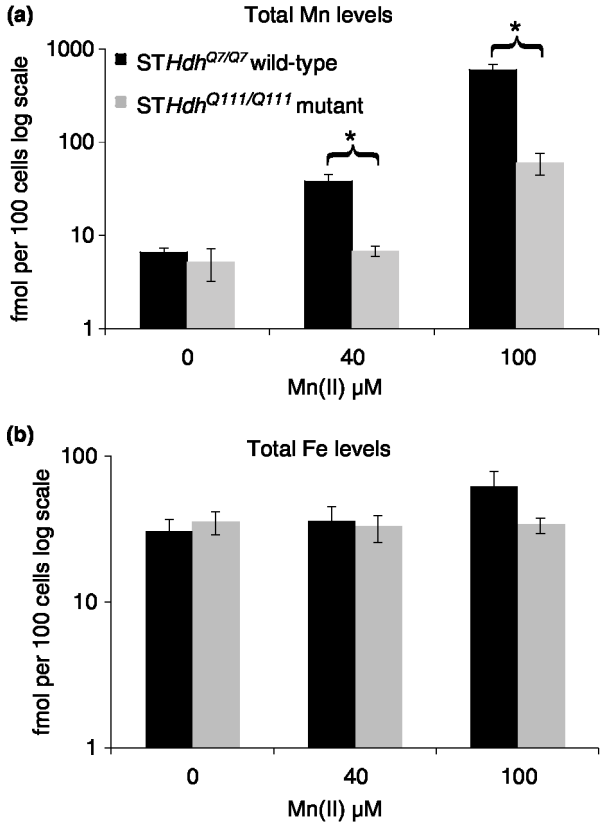

Fig. 6 Substantial decrease in manganese accumulation in HD striatal cells. Measurement of total intracellular manganese in (black) ST*Hdh*$^{Q7/Q7}$ or (gray) ST*Hdh*$^{Q111/Q111}$ cell lines after application of indicated concentrations of Mn(II) chloride for 30 h. (a) The average amount of intracellular manganese is plotted on log scale (± SEM, $n = 5$ independent samples). (b) Measurement of total intracellular iron levels after application of Mn(II) chloride for 30 h. The average amount of intracellular iron is plotted on log scale (± SEM, $n = 5$ independent samples). Significant differences in metal levels (*$p < 0.05$ *post hoc t*-test) between wild-type and mutant ST*Hdh* cells for each exposure are indicated.

Discussion

Our study has used a disease-toxicant interaction screen to evaluate toxicants that may share pathophysiological mechanisms underlying HD neurodegenerative processes. The approach exploited the diverse toxicology of metals to reveal processes that may underlie gene–environment interactions in disease. Metals were the toxicant of choice for this screen because they are known to alter cellular pathways also implicated in HD pathology. We tested eight metals and the mitochondrial complex II inhibitor 3NPA for modification of cell survival in the presence of either wild-type htt or a polyglutamine-expanded form of the protein. 3NPA was a positive control showing increased toxicity in the presence of the glutamine-expansion as previously reported (Fig. S1). The wild-type and HD mutant cell lines showed no difference in their response to the metals Cu(II), Fe(III), Pb(II), Co(II), Ni(II), or Zn(II) (Fig. 1). In contrast, the mutant HD cell line was found to have enhanced sensitivity to Cd(II) toxicity, and resistance to Mn(II) toxicity. The selective effect of these two metals strongly suggests that the HD mutation can alter the influence of specific environmental toxicants on striatal neurons and validates the utility of a disease-toxicant interaction screen to identify pathways of gene–environment interactions.

Oxidative stress is known to be a key factor in copper and iron mediated toxicity and is a potential mechanism of HD pathology. The lack of a significant difference in toxicity between genotypes with these metals is consistent with an earlier study that found no difference in vulnerability to oxidative stress in another HD cell model (Fig. 1) (Snider et al. 2003). Furthermore, it suggests that a change in sensitivity to oxidative stress is not

the source of the altered vulnerability of mutant STHdh$^{Q111/Q111}$ cells to cadmium, manganese or 3NPA (Figs 1 and S1).

Cadmium and 3NPA exert their toxic effects directly on the mitochondria (Li et al. 2003; Mao et al. 2006). The mutant STHdh$^{Q111/Q111}$ cells are reported to have an increased susceptibility to multiple mitochondrial stressors (Gines et al. 2003b; Seong et al. 2005; Oliveira et al. 2006). More recently, Cd(II) toxicity has been linked to aberrant activation of mitogen-activated protein kinases and the mammalian target of rapamycin cell signaling pathways (Lopez et al. 2006; Chen et al. 2008). Disruption of these signaling pathways has also been suggested in HD (Ravikumar et al. 2004; Apostol et al. 2006). Further investigation is needed to determine the relative contribution of these and other mechanisms to the increased sensitivity of STHdh$^{Q111/Q111}$ cells to Cd(II) toxicity.

Activation of Akt via S473 phosphorylation has been associated with neuroprotection (Brunet et al. 2001). Yet, we found that the increased sensitivity of mutant STHdh$^{Q111/Q111}$ cells to Cd(II) toxicity correlated with increased S473-P-Akt levels relative to wild-type exposed cells, while the decreased sensitivity to Mn(II) toxicity correlated with a blunted S473-PAkt response. While this observation does not rule out a neuroprotective role for Akt signaling in Mn(II) or Cd(II) toxicity, it does demonstrate that enhanced Akt activation between wild-type and HD mutant cells does not correlate with improved cell survival following exposure to these environmental toxicants in the STHdh cellular model. Future studies are needed to explore changes in Akt signaling following exposure to these metals in animal models of HD. Besides Akt, several other kinases are reported to be activated upon Mn(II) exposure including extracellular signal-regulated kinase, p38, and c-Jun N-terminal kinase (Bae et al. 2006; Moreno et al. 2008; Lee et al. 2009). Additionally, Cd(II) has been shown to affect mitogen-activated protein kinase/extracellular signal-regulated kinase signaling in hippocampal slices (Rigon et al. 2008). It will be interesting to evaluate how HD influences activation of these and other signaling systems that are modulated by Mn(II) and Cd(II).

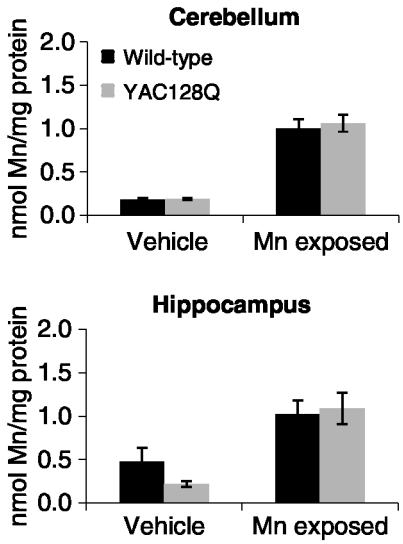

Fig. 7 Reduced striatal manganese uptake in the YAC128Q HD mouse model. Wild-type and YAC128Q HD mice at 3 months of age were exposed to Mn(II) by subcutaneous injection on Days 0, 3, and 7. Brain regions, tails, and whole blood were harvested on Day 8, and total manganese levels per mg of protein were determined by GFAAS. Mean manganese levels ± SEM are shown (n = 12–14 samples for each genotype-exposure group; 53 animals total). Total iron levels are shown in Fig. S3; ANOVA analysis of total manganese levels showed a significant effect of Mn(II) exposure for

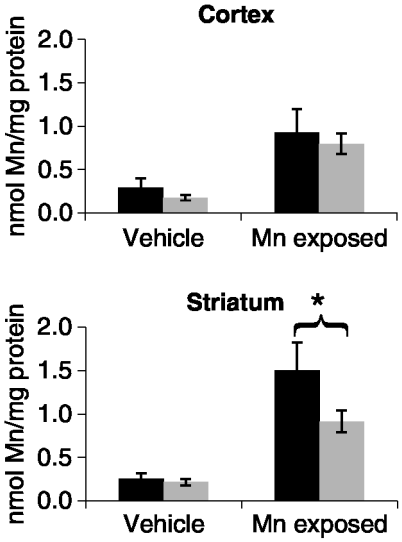

all four brain regions ($p < 0.05$). A significant genotype and genotype by Mn(II) exposure two-way interaction was found for the striatum only ($p < 0.05$). *Post hoc* analysis of the exposure effect showed a significant increase in manganese levels in Mn(II)-exposed animals compared with vehicle-only animals of the same genotype ($p < 0.05$ *post hoc t*-test, not indicated). *Post hoc* analysis of the genotype effect found a significant difference in striatal manganese accumulation between wild-type and mutant animals as indicated (*$p < 0.05$ *post hoc t*-test).

We report the discovery that expression of the disease-causing allele of htt suppresses Mn(II) toxicity (Figs 1, 2, and 4). This neuroprotective interaction was highly metal specific, suggesting a unique relationship between mutant htt and Mn(II) toxicity. We found no evidence that htt protein levels are altered by 40 µM Mn(II) exposure, indicating that survival differences between cells does not depend on changes in the expression of the toxic mutant htt protein. However, it remains possible that higher levels of Mn(II) exposure may be able to alter the expression of htt. Importantly, dosimetry studies have revealed that manganese concentrations in rodent striatum are normally between 4 and 18 µM, and can increase to as high as 70 µM in Mn(II) exposed animals (Aschner et al. 2005). Thus, our observation of a htt-manganese gene–environment interaction at Mn(II) exposures in this range are potentially pathologically relevant. Further work is needed to evaluate the relationship between manganese homeostasis and HD.

The significant decrease in net manganese accumulation in the mutant cells justifies the strong Mn(II) resistance phenotype, and suggests a manganese homeostatic defect because of mutant HTT. Of particular note, a comparison of cell survival and total manganese accumulation reveals that wild-type cells exposed to 40 µM Mn(II) have statistically indistinguishable cell survival and total manganese levels relative to mutant cells exposed at 100 µM Mn(II) (Figs 2 vs. 6a). These data strongly suggest that impairment in manganese accumulation may contribute, at least in part, to the Mn(II) resistance phenotype of STHdh$^{Q111/Q111}$ cells. Furthermore, the cellular disease-toxicant interaction accurately predicted a defect in manganese accumulation in the striatum of the YAC128Q HD mouse model. Indeed, the in vivo study showed a manganese-accumulation deficit in the very brain region most vulnerable in HD (Fig. 7). However, additional work is needed to determine if the specific nature of the manganese-accumulation defect is similar between the cellular and animal models (e.g. extracellular vs. intracellular accumulation). We propose three possible general mechanisms for the deficient manganese accumulation in the mutant STHdh$^{Q111/Q111}$ cells: (i) a decrease in manganese uptake, (ii) an increase in manganese export, and (iii) a decrease in manganese storage capacity. Future studies will explore the kinetics of the manganese transport defect to elucidate the cellular mechanism and transporters involved.

Supporting information

Additional Supporting information may be found in the online version of this article:

Fig. S1 Survival curve for 3NPA cytotoxicity in wild-type versus HD striatal cell lines.
Fig. S2 Diminished manganese-dependent Akt phosphorylation in HD striatal cells normalized wild-type vehicle control.
Fig. S3 Iron levels in Mn(II)-exposed animals.
Table S1 Analysis of regional manganese levels by multivariate two-way ANOVA
Table S2 Analysis of regional iron levels by multivariate two-way ANOVA

References

Anderson J. G., Fordahl S. C., Cooney P. T., Weaver T. L., Colyer C. L. and Erikson K. M. (2009) Extracellular norepinephrine, norepinephrine receptor and transporter protein and mRNA levels are differentially altered in the developing rat brain due to dietary iron deficiency and manganese exposure. Brain Res. 1281, 1–14.
Apostol B. L., Illes K., Pallos J. et al. (2006) Mutant huntingtin alters MAPK signaling pathways in PC12 and striatal cells: ERK1/2 protects against mutant huntingtin-associated toxicity. Hum. Mol. Genet. 15, 273–285.
Aschner M., Erikson K. M. and Dorman D. C. (2005) Manganese dosimetry: species differences and implications for neurotoxicity. Crit. Rev. Toxicol. 35, 1–32.
Bae J. H., Jang B. C., Suh S. I., Ha E., Baik H. H., Kim S. S., Lee M. Y. and Shin D. H. (2006) Manganese induces inducible nitric oxide synthase (iNOS) expression via activation of both MAP kinase and PI3K/Akt pathways in BV2 microglial cells. Neurosci. Lett. 398, 151–154.
Beal M. F., Brouillet E., Jenkins B. G. et al. (1993) Neurochemical and histologic characterization of striatal excitotoxic lesions produced by the mitochondrial toxin 3-nitropropionic acid. J. Neurosci. 13, 4181–4192.
Bowman A. B., Lam Y. C., Jafar-Nejad P. et al. (2007) Duplication of Atxn1l suppresses SCA1 neuropathology by decreasing incorporation of polyglutamine-expanded ataxin-1 into native complexes. Nat. Genet. 39, 373–379.
Brunet A., Datta S. R. and Greenberg M. E. (2001) Transcription-dependent and -independent control of neuronal survival by the PI3K-Akt signaling pathway. Curr. Opin. Neurobiol. 11, 297–305.
Bush A. I. (2000) Metals and neuroscience. Curr. Opin. Chem. Biol. 4, 184–191.
Cattaneo E. and Conti L. (1998) Generation and characterization of embryonic striatal conditionally immortalized ST14A cells. J. Neurosci. Res. 53, 223–234.
Chen L., Liu L., Luo Y. and Huang S. (2008) MAPK and mTOR pathways are involved in cadmium-induced neuronal apoptosis. J. Neurochem. 105, 251–261.
Colin E., Regulier E., Perrin V., Durr A., Brice A., Aebischer P., Deglon N., Humbert S. and Saudou F. (2005) Akt is altered in an animal model of Huntington's disease and in patients. Eur. J. Neurosci. 21, 1478–1488.
Dexter D. T., Carayon A., Javoy-Agid F., Agid Y., Wells F. R., Daniel S. E., Lees A. J., Jenner P. and Marsden C. D. (199 1) Alterations in the levels of iron, ferritin and other trace metals in Parkinson's disease and other neurodegenerative diseases affecting the basal ganglia. Brain 114(Pt. 4), 1953–1975.
Dodd C. A., Ward D. L. and Klein B. G. (2005) Basal Ganglia accumulation and motor assessment following manganese chloride exposure in the C57BL/6 mouse. Int. J. Toxicol. 24, 389–397.
Ehrich M. and Sharova L. (2000) In vitro methods for detecting cytotoxcity. Curr. Protoc. Toxicol. 3, 6.2.11–6.2.12.
Fox J. H., Kama J. A., Lieberman G. et al. (2007) Mechanisms of copper ion mediated Huntington's disease progression. PLoS ONE 2, e334.
Garcia S. J., Gellein K., Syversen T. and Aschner M. (2007) Iron deficient and manganese supplemented diets alter metals and transporters in the developing rat brain. Toxicol. Sci. 95, 205–214.
Gines S., Ivanova E., Seong I. S., Saura C. A. and MacDonald M. E. (2003a) Enhanced Akt signaling is an early pro-survival response that reflects N-methyl-D-aspartate receptor activation in Huntington's disease knock-in striatal cells. J. Biol. Chem. 278, 50514– 50522.
Gines S., Seong I. S., Fossale E., Ivanova E., Trettel F., Gusella J. F., Wheeler V. C., Persichetti F. and MacDonald M. E. (2003b) Specific progressive cAMP reduction implicates energy deficit in presymptomatic Huntington's disease knock-in mice. Hum. Mol. Genet. 12, 497–508.

Hilditch-Maguire P., Trettel F., Passani L. A., Auerbach A., Persichetti F. and MacDonald M. E. (2000) Huntingtin: an iron-regulated protein essential for normal nuclear and perinuclear organelles. Hum. Mol. Genet. 9, 2789–2797.
Humbert S., Bryson E. A., Cordelieres F. P., Connors N. C., Datta S. R., Finkbeiner S., Greenberg M. E. and Saudou F. (2002) The IGF-1/Akt pathway is neuroprotective in Huntington's disease and involves Huntingtin phosphorylation by Akt. Dev. Cell 2, 831–837.
Imarisio S., Carmichael J., Korolchuk V. et al. (2008) Huntington's disease: from pathology and genetics to potential therapies. Biochem. J. 412, 191–209.
Kreutz C., Bartolome Rodriguez M. M., Maiwald T., Seidl M., Blum H. E., Mohr L. and Timmer J. (2007) An error model for protein quantification. Bioinformatics 23, 2747–2753.
Lee E. S., Yin Z., Milatovic D., Jiang H. and Aschner M. (2009) Estrogen and tamoxifen protect against Mn-induced toxicity in rat cortical primary cultures of neurons and astrocytes. Toxicol. Sci. 110, 156–167.
Li M., Xia T., Jiang C. S., Li L. J., Fu J. L. and Zhou Z. C. (2003) Cadmium directly induced the opening of membrane permeability pore of mitochondria which possibly involved in cadmium-triggered apoptosis. Toxicology 194, 19–33.
Liao S. L., Ou Y. C., Chen S. Y., Chiang A. N. and Chen C. J. (2007) Induction of cyclooxygenase-2 expression by manganese in cultured astrocytes. Neurochem. Int. 50, 905–915.
Lopez E., Arce C., Oset-Gasque M. J., Canadas S. and Gonzalez M. P. (2006) Cadmium induces reactive oxygen species generation and lipid peroxidation in cortical neurons in culture. Free Radic. Biol. Med. 40, 940–951.
Mao Z., Choo Y. S. and Lesort M. (2006) Cystamine and cysteamine prevent 3-NP-induced mitochondrial depolarization of Huntington's disease knock-in striatal cells. Eur. J. Neurosci. 23, 1701–1710.
Moreno J. A., Sullivan K. A., Carbone D. L., Hanneman W. H. and Tjalkens R. B. (2008) Manganese potentiates nuclear factor-kappaB-dependent expression of nitric oxide synthase 2 in astrocytes by activating soluble guanylate cyclase and extracellular responsive kinase signaling pathways. J. Neurosci. Res. 86, 2028–2038.
Oliveira J. M., Chen S., Almeida S. et al. (2006) Mitochondrialdependent Ca^{2+} handling in Huntington's disease striatal cells: effect of histone deacetylase inhibitors. J. Neurosci. 26, 11174– 11186.
Ravikumar B., Vacher C., Berger Z. et al. (2004) Inhibition of mTOR induces autophagy and reduces toxicity of polyglutamine expansions in fly and mouse models of Huntington disease. Nat. Genet. 36,585–595.
Rigon A. P., Cordova F. M., Oliveira C. S. et al. (2008) Neurotoxicity of cadmium on immature hippocampus and a neuroprotective role for p38 MAPK. Neurotoxicology 29, 727–734.
Ruan Q., Lesort M., MacDonald M. E. and Johnson G. V. (2004) Striatal cells from mutant huntingtin knock-in mice are selectively vulnerable to mitochondrial complex II inhibitor-induced cell death through a non-apoptotic pathway. Hum. Mol. Genet. 13, 669–681.
Seong I. S., Ivanova E., Lee J. M. et al. (2005) HD CAG repeat implicates a dominant property of huntingtin in mitochondrial energy metabolism. Hum. Mol. Genet. 14, 2871–2880.
Simmons D. A., Casale M., Alcon B., Pham N., Narayan N. and Lynch G. (2007) Ferritin accumulation in dystrophic microglia is an early event in the development of Huntington's disease. Glia 55, 1074– 1084.
Slow E. J., van Raamsdonk J., Rogers D. et al. (2003) Selective striatal neuronal loss in a YAC128 mouse model of Huntington disease. Hum. Mol. Genet. 12, 1555–1567.
Snider B. J., Moss J. L., Revilla F. J., Lee C. S., Wheeler V. C., Macdonald M. E. and Choi D. W. (2003) Neocortical neurons cultured from mice with expanded CAG repeats in the huntingtin gene: unaltered vulnerability to excitotoxins and other insults. Neuroscience 120, 617–625.
Thevenod F. (2009) Cadmium and cellular signaling cascades: to be or not to be? Toxicol. Appl. Pharmacol. 238, 221–239.
Trettel F., Rigamonti D., Hilditch-Maguire P., Wheeler V. C., Sharp A. H., Persichetti F., Cattaneo E. and MacDonald M. E. (2000) Dominant phenotypes produced by the HD mutation in STHdh(Q111) striatal cells. Hum. Mol. Genet. 9, 2799–2809.
Warby S. C., Chan E. Y., Metzler M., Gan L., Singaraja R. R., Crocker S. F., Robertson H. A. and Hayden M. R. (2005) Huntingtin phosphorylation on serine 421 is significantly reduced in the striatum and by polyglutamine expansion in vivo. Hum. Mol. Genet. 14, 1569–1577.

Ying H. S., Gottron F. J. and Choi D. W. (2000) Assessment of cell viability in primary neuronal cultures. Curr. Protoc. Neurosci. 13, 7.18.8–7.18.9.
Zecca L., Youdim M. B., Riederer P., Connor J. R. and Crichton R. R. (2004) Iron, brain ageing and neurodegenerative disorders. Nat. Rev. Neurosci. 5, 863–873.
Zheng W., Zhao Q., Slavkovich V., Aschner M. and Graziano J. H. (1999) Alteration of iron homeostasis following chronic exposure to manganese in rats. Brain Res. 833, 125–132.